

Synthesis and Structure of Four-Coordinate Copper(II) Complexes Stabilized by β -Ketiminato Ligands and Application in the Reverse Atom-Transfer Radical Polymerization of Styrene

Stefano Gulli,^[a] Jean-Claude Daran,^[a] and Rinaldo Poli*^[a,b]

Keywords: Copper / Functionalized ligands / Radical reactions / Polymerization / Polystyrene

The reaction of CuCl_2 with $\text{R}_2\text{NCH}_2\text{CH}_2\text{NHC}(\text{Me})=\text{CHCO}(\text{Me})$ [$\text{R} = \text{Me}$ (HL^1) or Et (HL^2)] in the presence of Et_3N leads to the formation of complexes $[\text{CuCl}(\text{L}^n)]$ [$n = 1$ (**1**), 2 (**2**)]. Whereas the solid-state structure of compound **2** is mononuclear with a close to square-planar arrangement of the ClON_2 donor set, compound **1** adopts a dinuclear di- μ -chlorido arrangement in which two mononuclear units having essentially the same arrangement as in **2** establish loose axial $\text{Cu}\cdots\text{Cl}$ interactions, each one of them with the Cl atom of the other one. Compounds **1** and **2** have been tested as reversible

trapping agents for the controlled radical polymerization of styrene under a reverse atom-transfer radical polymerization (ATRP) approach. Reversible Cl atom transfer leading to a controlled polymerization process is observed, although the controllability is negatively affected by slow radical trapping. A moderate effect on the polymerization rate, once all the radical initiator is consumed, was observed in the presence of an excess amount of pyridine (10 equiv. per Cu) and interpreted on the basis of the stabilization of the Cu^{I} system.

Introduction

Copper coordination chemistry with multidentate ligands has recently experienced a revival after the discovery^[1] and intensive development^[2–5] of Cu-mediated controlled radical polymerization. This polymerization strategy rests on the reversible trapping of the growing radical chain, which is accomplished by transfer of a halogen atom from a $\text{Cu}^{\text{II}}\text{--X}$ compound, to yield the corresponding Cu^{I} complex and the halogen-terminated radical chain. The technique is therefore named “atom-transfer radical polymerization” (ATRP). The process can be started from stable Cu^{I} complexes, usually made in situ from CuX ($\text{X} = \text{Cl}$ or Br) and a suitable multidentate ligand, plus a halogenated compound R--X as initiator, in the presence of the polymerizable monomer (so-called ATRP conditions). Alternatively, it can be started from a stable Cu^{II} complex (also usually made in situ from CuX_2 and the appropriate ligand) and a standard radical source, in the presence of the monomer (so-called reverse ATRP conditions).

A recent review, focused on the structural aspects of copper-catalyzed ATRP, shows that the complexes used for this purpose are inevitably made by mixing CuX and CuX_2 with neutral supporting ligands, therefore always containing a halogen atom in the coordination sphere.^[6] Occasionally, the halide is displaced to yield cationic complexes, such as for instance $[\text{Cu}(\text{bipy})_2]^+_{[7]}$ ($\text{bipy} = 2,2'$ -bipyridine) or $[\text{Cu}\{\text{Me}_6(\text{tren})\}]^+_{[8]}$ [$\text{tren} = \text{tris}(2\text{-aminoethyl})\text{amine}$],^[8] but the introduction of the anionic functionality into the multidentate ligand itself does not seem to have so far attracted much attention. We wish to explore here the use of anionic multidentate ligands for copper coordination chemistry, starting with the tridentate “ XL_2 ” type. This is the minimum denticity likely to provide stable complexes in both oxidation states, since the $[\text{Cu}^{\text{II}}\text{Cl}(\text{XL}_2)]$ coordination environment is well established, for instance in $[\text{Tp}^*\text{CuCl}]$ [$\text{Tp}^* = \text{tris}(3,5\text{-dimethylpyrazolyl})\text{borate}$],^[9] and the putative three-coordinate $[\text{Cu}^{\text{I}}\text{XL}_2]$ system resulting from the halogen atom transfer may be stabilized by dimerization or by monomer coordination, as for instance in $[\text{Tp}^*\text{Cu}]_2$ or $[\text{Tp}^*\text{Cu}(\text{olefin})]$ complexes.^[10,11]

One of the simplest ways to introduce an anionic functionality in a chelating ligand is through deprotonation of a β -diketone such as acetylacetone. Since Cu has higher affinity to N ligands, modification of acetylacetone by introduction of a diamine was envisaged to yield amine-functionalized β -ketimines, a well-known class of ligands that has already been used to generate Cu^{I} derivatives.^[12–15] We report here the synthesis and structural characterization of new copper(II) complexes incorporating these ligands, as

[a] CNRS, LCC (Laboratoire de Chimie de Coordination), Université de Toulouse, UPS, INPT
205, route de Narbonne, 31077 Toulouse, France
Fax: +33-5-61553003
E-mail: rinaldo.poli@lcc-toulouse.fr
Homepage: http://www.lcc-toulouse.fr/equipe_g/pages/poli/index.html

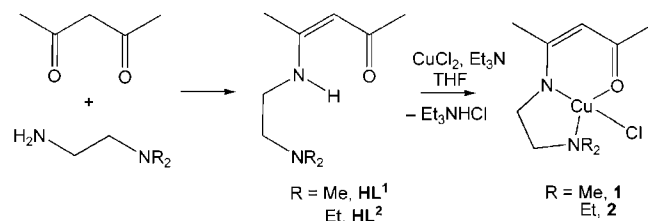
[b] Institut Universitaire de France
103, bd Saint-Michel, 75005 Paris, France

Supporting information for this article is available on the WWW under <http://dx.doi.org/10.1002/ejic.201001203>.

well as a preliminary exploration of their ability to control the radical polymerization of styrene under reverse ATRP conditions.

Results and Discussion

Condensation of acetylacetone with 1 equiv. of $R_2NCH_2CH_2NH_2$ ($R = \text{Me}, \text{Et}$) yielded ligands HL^1 and HL^2 as shown in Scheme 1.^[16–19] Both ligands have recently been used in coordination chemistry with both main group^[17,19] and transition metals.^[12,15,20] The reaction of these ligands with anhydrous CuCl_2 in THF, in the presence of triethylamine (1 equiv), provides a high-yield entry into complexes $[\text{CuCl}(\text{L}^1)]$ (**1**) and $[\text{CuCl}(\text{L}^2)]$ (**2**).



Scheme 1.

Complex **2** has already been recently described.^[12] It was synthesized in unreported yields by direct interaction of CuCl_2 and HL^2 in acetone at 60–65 °C without use of a base, and it was only characterized by IR spectroscopy. Our method uses NEt_3 , allowing the elimination of the generated HCl as Et_3NHCl , which precipitates in THF and can be easily removed by filtration, while the reaction at room temperature is complete in less than 2 h. Solutions of the two compounds in dichloromethane show a sharp EPR spectrum at room temperature (Figure 1a), with the expected 1:1:1:1 hyperfine splitting caused by the $I = 3/2$ Cu nucleus. The diethylamino derivative **2** also reveals an additional and barely discernible superhyperfine splitting, which may be caused by coupling to one of the N atoms (^{14}N : $I = 1$). The g tensor is tetragonal, as revealed by the spectrum taken at 120 K (Figure 1b), with a large a_{\parallel} and a nondiscernible a_{\perp} .

Both complexes have been structurally characterized by X-ray diffraction. The structural chemistry of these molecules presents an interesting feature related to the nuclearity. Compound **2** is mononuclear and four-coordinate, with a close to square-planar coordination geometry (Figure 2). When considering the plane of the electronically delocalized $\text{Cu}(\beta\text{-ketiminato})$ moiety, the donor N atom of the Et_2N moiety deviates only slightly [0.203(2) Å] on one side of the plane, whereas the Cl atom deviates to a larger extent [0.933(1) Å] in the other direction. The trans-N1-Cu-Cl angle is significantly smaller than 180° [163.62(4)°], but the O-Cu-N2 angle is also rather small. The Cl-Cu-O plane makes a dihedral angle of 21.47(7)° with the N1-Cu-N2 plane. This distortion appears quite natural for this specific coordination environment. A search of the Cambridge Structural Database for other four-coordinate Cu com-

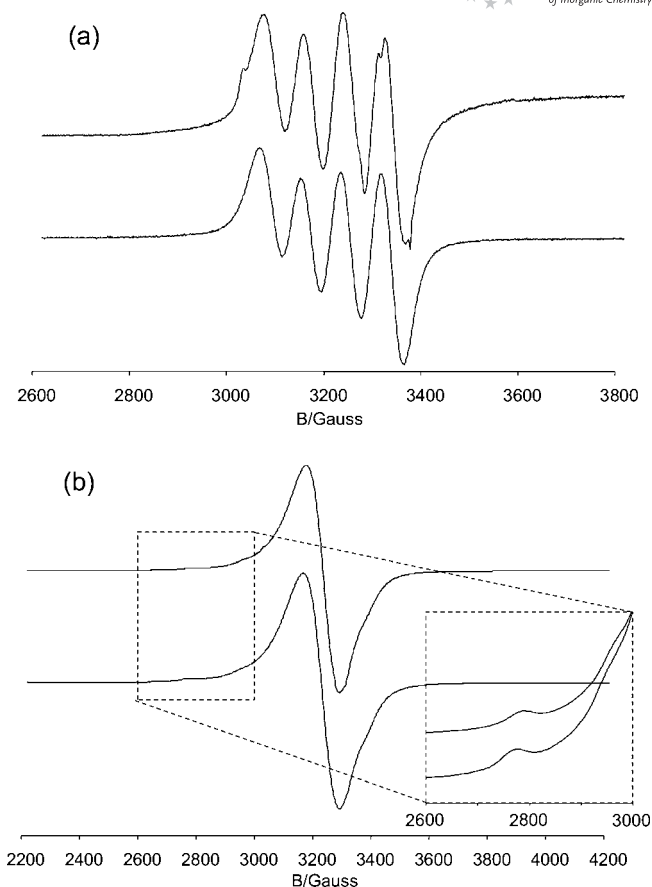


Figure 1. EPR spectra of solutions of compounds **1** (bottom) and **2** (top) in CH_2Cl_2 : (a) at room temperature and (b) at 120 K.

plexes with a ClON_2 donor set has revealed 42 mononuclear geometries, for which the average value of this specific dihedral angle is $(11 \pm 7)^\circ$.

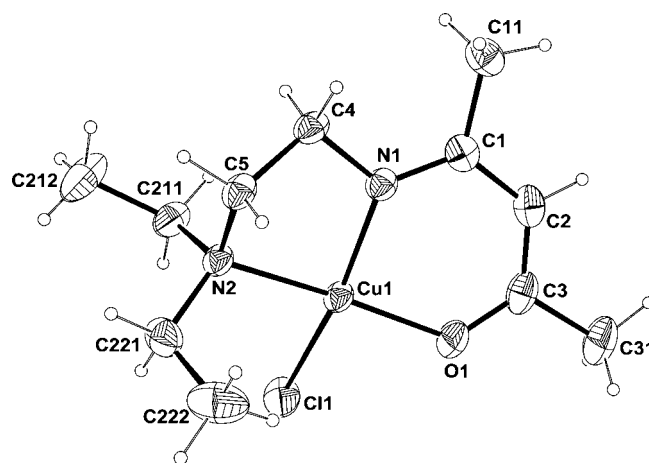


Figure 2. ORTEP view of a molecule of compound **2**, also showing the numbering scheme used. Thermal ellipsoids are drawn at the 50% probability level. Main geometrical parameters: Cu–Cl 2.2458(4), Cu–O 1.9126(10), Cu–N1 1.9404(12), Cu–N2 2.0563(12) Å; Cl–Cu–O 91.92(4), Cl–Cu–N1 163.62(4), Cl–Cu–N2 93.46(4), O–Cu–N1 92.92(5), O–Cu–N2 166.32(5), N1–Cu–N2 85.38(5)°.

Compound **1**, on the other hand, is dinuclear, with bridging Cl atoms and five-coordinate Cu centers (Figure 3). The bridging Cu_2Cl_2 moiety is in fact quite asymmetric, with very different Cu–Cl distances. The shorter Cu–Cl distance is only slightly lengthened relative to the Cu–Cl distance in compound **2**. Upon closer examination, it is clear that the compound can be described as the dimerization of $[\text{CuCl}(\text{L}^1)]$ moieties that have a geometry very closely related to that of the mononuclear compound **2**, through loose $\text{Cu}-\text{Cl}^i$ and Cu^i-Cl interactions. Indeed, the coordination geometries around the Cu center in **1** and **2** are strikingly similar, including the deviation of the Cl–Cu–N1 angle from linearity and the dihedral angle between the N1–Cu–N2 and Cl–Cu–O planes from coplanarity [15.19(6)°].

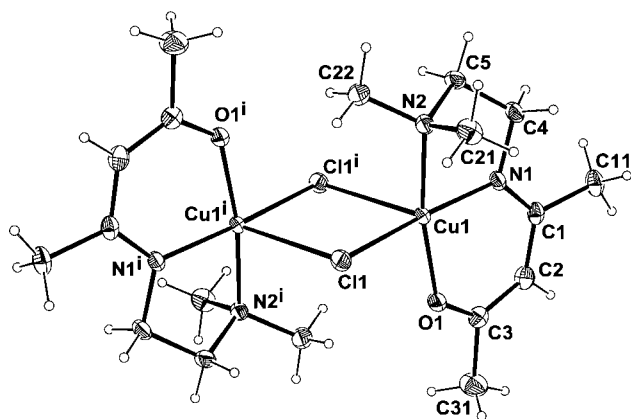


Figure 3. ORTEP view of a molecule of compound **1**, also showing the numbering scheme used. Thermal ellipsoids are drawn at the 50% probability level. Main geometrical parameters: Cu–Cl 2.3202(4), Cu–Clⁱ 2.8442(4), Cu–O 1.917(1), Cu–N1 1.9642(13), Cu–N2 2.0610(13) Å; Cl–Cu–Clⁱ 85.77(1), Cl–Cu–O 88.97(3), Cl–Cu–N1 170.47(4), Cl–Cu–N2 92.65(4), Clⁱ–Cu–O 97.56(4), Clⁱ–Cu–N1 103.40(4), Clⁱ–Cu–N2 95.25(4), O–Cu–N1 92.34(5), O–Cu–N2 167.17(5), N1–Cu–N2 84.02(5)°. Symmetry code: ⁱ 1 – *x*, –*y*, 1 – *z*.

An interesting question therefore arises: why this nuclearity difference? The existence of the Cu–Clⁱ interactions demonstrates the preference for a dinuclear structure, but their weakness suggests that their establishment may be discouraged by small perturbations. For compound **2**, for which the shortest intermolecular contacts of the Cl atom are established with C–H bonds of neighboring (diethylamino)ethyl moieties, the small perturbation is undoubtedly caused by the steric repulsion that the ethyl substituents would experience in a dinuclear structure. Indeed, the space-filling model of compound **1**, shown in Figure 4, indicates how one of the NMe₂ methyl groups in one half of the molecule (right arrow) finds itself in close proximity with the methyl group of the keto group in the other half of the molecule (left arrow), thereby suggesting that a similar structure may not be sufficiently favored with the bulkier NEt₂-substituted ligand. It is then also interesting to re-examine the related mononuclear Cu structures that contain a ClON₂ ligand set already described in the literature to identify the perturbation that impedes dimerization in those cases.

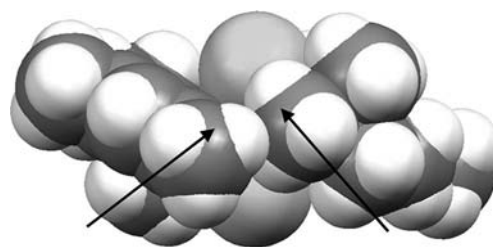


Figure 4. Space-filling view of the structure of compound **1**.

For a few compounds, the authors reported a four-coordinate structure without realizing the presence of a loose axial interaction with an interstitial solvent molecule. This is the case for a few “methanol solvates,” with Cu–O distances to the axially bonded MeOH ligand as small as 2.27 Å.^[21–23] For another three compounds, the structure was described as mononuclear but it is in fact halide-bridged dinuclear, just like **1**, with “loose” Cu–X distances of 2.61^[24] and 2.84 Å^[25] (X = Cl), or 3.09 Å^[26] (X = Br). In other cases, although axial donor atoms are too far away for detection as bonding interactions (the distance is longer than the sum of van der Waals radii), the donor atom (Cl but sometimes also O) is correctly positioned to provide some axial electron density to the Cu center in 2D or 3D packing arrangements.^[27–32] Interesting situations are presented by other structures that, like compound **2**, are genuinely mononuclear, without significant additional contacts to the four-coordinate Cu^{II} center. A few of these are polyaromatic compounds with delocalized planar ligands, which always display a π -stacking arrangement.^[33–40] This indicates that intermolecular π -stacking interactions provide better stabilization to the crystal structure than the halide-bridge formation. In other cases, the dinuclear structure simply does not form because of the presence of a bulky group near the Cu center, either an NEt₂ group like in compound **2**,^[41,42] or another bulky group.^[31,43,44]

The structure of compound **1** is identical to that of compound $[\text{Cu}(\text{L}^1)(\text{O}_2\text{CPh})_2]$,^[15] in which the benzoate ligand occupies the same position as the Cl ligand in **1** by adopting a bridging monodentate ($\kappa^1:\mu$) coordination mode, also with very different distances to the two Cu atoms [1.984(2) Å for the strong equatorial bond, 2.788 Å for the loose axial bond]. The Cu–N2 bond [2.064(3) Å] is essentially identical to that in **1**, whereas the Cu–N1 bond [1.914(3) Å] is significantly shorter, and the Cu–O1 [1.944(3) Å] is significantly longer. The structure of **2**, on the other hand, may be directly compared with that of $[\text{CuCl}\{\text{Et}_2\text{NCH}_2\text{CH}_2\text{NC}(\text{Me})\text{CHC}(\text{Ph})\text{O}\}]$; the two compounds differ only by the nature of the substituent at the keto position (Ph vs. Me).^[31] In the Ph-substituted compound, the Cu–Cl distance is significantly longer (2.300 Å), whereas the Cu–N1 distance (1.956 Å) is marginally longer, and the Cu–O (2.107 Å) and Cu–N2 (1.992 Å) distances are marginally shorter. The *trans*-Cl–Cu–N1 angle (164.8°) is quite similar to that in **1**.

Compounds **1** and **2** have been tested as controlling agents for the radical polymerization of styrene under re-

verse ATRP conditions. The first experiments carried out at 80 °C, with primary radicals generated from 2,2'-azobis(isobutyronitrile) (AIBN; $t_{1/2} \approx 70$ min), are shown in Figure 5a.

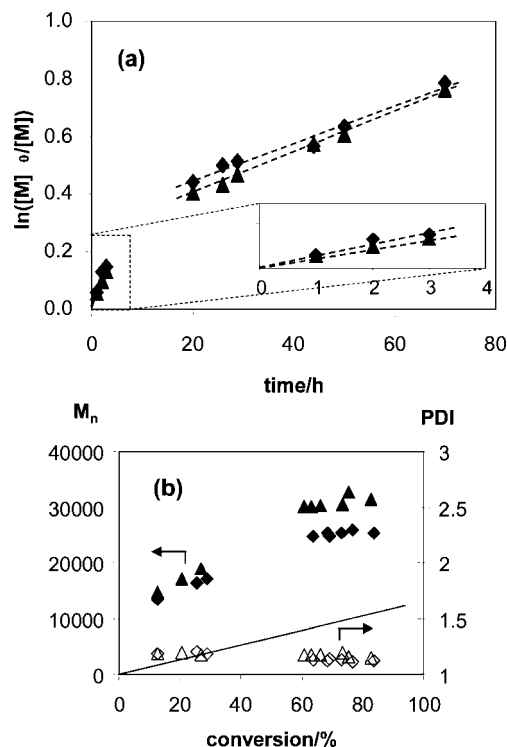


Figure 5. (a) First-order kinetic plot, and (b) M_n (filled symbols) and polydispersity index (PDI; empty symbols) versus conversion for the radical polymerization of styrene in the presence of compounds **1** (triangles) or **2** (diamonds). The straight line in plot (b) indicates the theoretical molecular weight $[M_{R^\bullet} + M_M \cdot (nM/n_{Cu}) \cdot p + M_{Cl}]$; for which M_{R^\bullet} , M_M , and M_{Cl} are the molar masses of primary radical, monomer, and Cl atom, respectively; p is the degree of conversion; and (nM/n_{Cu}) is the molar ratio of monomer and Cu]. Conditions: 50% (v/v) in toluene, 80 °C, [styrene]/[AIBN]/[Cu] = 200:0.8:1.

Several features of the two plots shown in Figure 5 deserve discussion. The first and most important one is that polymerization occurs and is sustained well beyond the time required to completely consume the radical initiator (6–7 h) in the presence of both compounds. Together with the continued increase of the number-average molecular weight and the low dispersities of the resulting polymers at high conversion, this offers evidence that the radical chains are continuously generated from a dormant species and that the polymerization is controlled. Note that the first-order kinetics plot indicates linearity in the high-conversion region (after completely consuming the initiator), which is in agreement with a constant radical concentration in solution and with the occurrence of the ATRP mechanism. At low conversions (short times), on the other hand, the polymerization is faster. In addition, the molecular weights at low conversions are much higher than the expected values, but subsequently continue to grow at approximately the expected growth rate, whereas the dispersity remains narrow throughout the polymerization process (< 1.2 ; see Fig-

ure 5b). This phenomenon can be ascribed to a slow trapping rate, thereby generating chains of much higher molecular weight than expected during the initial phase of initiator decomposition. The relatively long initial phase of initiator decomposition (6–7 half-lives, namely, 6–7 h) entails the continuous generation of new radical chains throughout this period, but the molecular-weight distribution does not appear to be too negatively affected by this initial phase of poor control.

The polymerization proceeds at approximately the same rate in the presence of compounds **1** and **2**, both before and after depletion of the radical initiator (see Figure 5a), thereby indicating that the activation/deactivation equilibrium is very similar for both copper compounds. In relation to the above-described structural study of the two Cu^{II} complexes, it is clear that the weak dichlorido-bridged interaction revealed for compound **1** does not play a major role in this process, as also indicated by the identical EPR spectroscopic properties of the two compounds in solution.

The putative Cu^I catalyst generated by Cl atom transfer to the radical chain is a three-coordinate complex in which the constraints of the ligand bite do not allow the metal center to adopt a preferred trigonal-planar configuration. Although, as mentioned in the Introduction, the complex may be stabilized by dimerization or by coordination of a monomer molecule, we wondered whether the addition of Lewis bases such as pyridine (py) or bipyridine (bipy) could affect the polymerization rate and controllability.

Because of the identical solution properties and polymerization results of compounds **1** and **2**, additional experiments in the presence of py or bipy were only carried out with the ethyl-substituted complex **2**. The results (Figure 6) indicate a negligible effect on the reaction rate when using only 1 equiv. of either additive. The difference between the three experiments may be considered to fall within the margins of experimental error. The trends of M_n and PDI as a function of conversion were also nearly identical for the three experiments. When the py/Cu ratio was increased to 10, however, the polymerization was significantly retarded in the second period, after full consumption of the initiator, whereas the behavior was once again identical before full consumption of the radical initiator. Therefore, it appears that the three-coordinate Cu^I complex generated by Cl atom transfer, $[Cu(L^2)]$, can be stabilized by the Lewis base additive as shown in Scheme 2, the overall effect being a shift of the deactivation equilibrium toward the Cu^I form. The absence of a notable effect on the rate during the first polymerization period is in agreement with the prediction that the Lewis additive action is restricted to the Cu^I stabilization and does not affect the rate of Cl atom transfer from compound **2** to the growing radical chain (deactivation, k_d).

An additional experiment was carried out in the presence of compound **2** and py (1 equiv.) at lower temperature (30 °C). In this case, 2,2'-azobis(4-methoxy-2,4-dimethylvaleronitrile) (V-70) was used as radical initiator ($t_{1/2} = 10$ h). The results are compared with those obtained at 80 °C in Figure 7. The polymerization rate is slower at 30 °C, as expected. Once again, the process is sustained be-

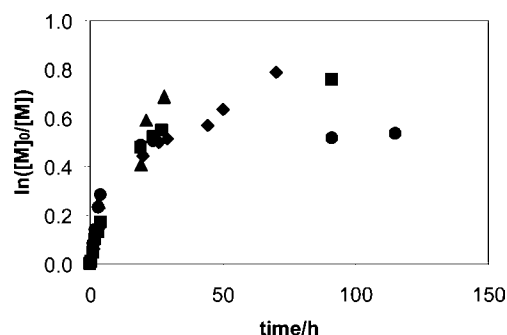
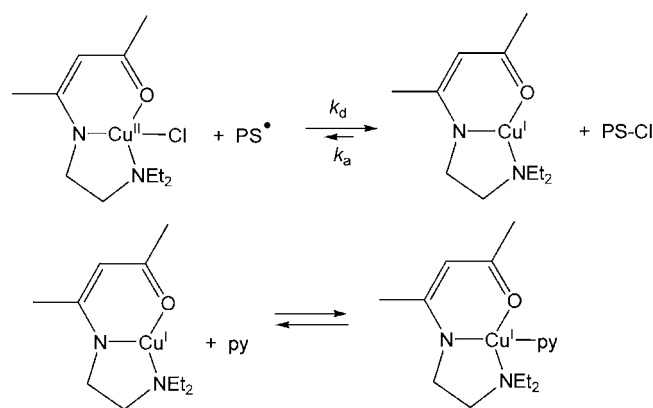


Figure 6. First-order kinetic plot for the radical polymerization of styrene in the presence of compound **2** alone (diamonds) or together with py (1 equiv., triangles; 10 equiv., spheres) or bipy (1 equiv., squares). Conditions are the same as in Figure 5.



Scheme 2.

yond the time needed to fully deplete the radical initiator (ca. 70 h for V-70 at 30 °C), with a visible breakpoint in the reaction rate, thereby indicating reversible reactivation of the dormant chains by atom transfer to Cu^I. However, the controllability is not improved, as shown by the fact that the polymer M_n is still large relative to the theoretical value, whereas the PDI is larger relative to the experimental value at 80 °C. The reason for this result is that, although controllability in the second polymerization period is expected to increase, the lower temperature also causes a slower deactivation rate, which negatively affects the molecular-weight distribution in the first polymerization period.

The slow radical trapping by complexes **1** and **2** may be directly related to the unsuitable geometry of the three-coordinate Cu^I species that is formed by Cl atom transfer. As has been previously pointed out, the best systems for rapid radical deactivation, which is crucial for good controllability, are those in which the coordination geometry changes in a minimal way on going from $L_n/Cu^{II}-Cl$ to L_n/Cu^I , whereas the electronic properties and the coordination geometry of the L_n coordination sphere are most suitable to the Cu^I species. In our case, the situation is quite the opposite, since the L¹ and L² ligands yield a suitable coordination environment for the Cu^{II} system in combination with the Cl atom but are not at all adapted to the Cu^I system.

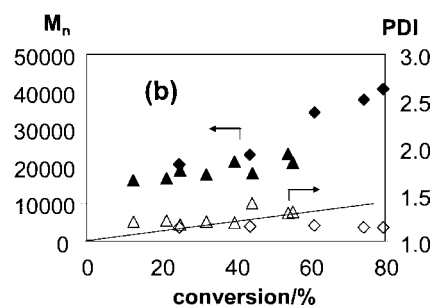


Figure 7. (a) First-order kinetic plot, and (b) M_n (filled symbols) and PDI (empty symbols) versus conversion for the radical polymerization of styrene in the presence of compound **2** and py (py/Cu = 1) at 80 °C (diamonds) and 30 °C (triangles). The straight line in plot (b) indicates the theoretical molecular weight [$M_{R^\bullet} + M_M \cdot (nM/n_{Cu}) \cdot p + M_{Cl}$]; for which M_{R^\bullet} , M_M , and M_{Cl} are the molar masses of primary radical, monomer, and Cl atom, respectively; p is the degree of conversion; and (nM/n_{Cu}) is the molar ratio of monomer and Cu]. Conditions for the experiment at 30 °C: 50% (v/v) in toluene, [styrene]/[V-70]/[Cu] = 200:0.8:1.

Conclusion

We have prepared and characterized two neutral four-coordinate Cu^{II} monochloride complexes. We disclose new structural features related to weak intermolecular Cu^{II}...Cl bonding and discuss the criteria that allow this interaction to occur in these and other related complexes previously described in the literature. These complexes have been tested as reversible trapping agents for growing polystyrene radical chains under reverse ATRP conditions. Whereas the systems are negatively affected by a slow trapping rate, the principle of reversible atom transfer that leads to a controlled radical polymerization has been demonstrated. The trapping rate is expected to be accelerated by using other tridentate “XL₂” ligands with larger bites, thus adapting to a trigonal-planar coordination for Cu^I, or perhaps even better by moving to a tetradentate “XL₃” ligand that would stabilize Cu^I in a tetrahedral environment. Research in our laboratory is now oriented along these directions.

Experimental Section

General: All solvents used in the reactions were distilled under argon. NMR spectra were recorded with Bruker ARX 250 and AV 300 instruments. Chemical shifts are expressed in ppm downfield from Me₄Si. EPR spectra were measured with a Bruker Elexsys E 500 spectrometer (X-band) equipped with both a frequency meter and a gauss meter. Acetylacetone, *N,N*-dimethylethylenediamine, *N,N*-diethylethylenediamine, and CuCl₂ were purchased from Sigma–Aldrich and used as received. Styrene (Sigma–Aldrich) was dehydrated by passing through a neutral alumina column and then stirred in the presence of CaH₂ for 1 d, followed by distillation under argon.

Synthesis of Me₂NCH₂CH₂NHC(Me)=CHC(Me)=O (HL¹): In a 500 mL round-bottomed flask equipped with a condenser, acetyl acetone (29.3 g, 0.29 mol) and *N,N*-dimethylethylenediamine (26 g, 0.29 mol) in benzene (250 mL) were heated to reflux for 48 h to yield an intense yellow solution. The conversion was monitored by measurement of the water removed from the reaction through a

Dean–Stark apparatus. The reaction started immediately, as suggested by the color change, but it was necessary to heat to reflux for 2 d to complete it. The solvent was then removed to yield an intense yellow liquid. Distillation at 115 °C yielded the product as a yellow oil. Yield: 47.1 g (95.5%). ^1H NMR (C_6D_6 , 250 MHz): δ = 11.1 [br. s, 1 H, NH], 4.98 (s, 1 H, $\text{CH}_3\text{CCHCCH}_3$), 2.93 (q, J = 6.2 Hz, 2 H, NHCH_2CH_2), 2.15 (t, J = 6.5 Hz, 2 H, NHCH_2CH_2), 2.08 (s, 3 H, CH_3CO), 2.06 [s, 6 H, $\text{N}(\text{CH}_3)_2$], 1.63 (s, 3 H, CH_3CN) ppm. ^{13}C NMR (C_6D_6 , 62.90 MHz): δ = 193.6, 161.5, 95.0, 58.9, 45.2, 40.9, 28.7, 18.4 ppm.

Synthesis of $\text{Et}_2\text{NCH}_2\text{CH}_2\text{NHC}(\text{Me})=\text{CHC}(\text{Me})=\text{O}$ (HL^2): In a 500 mL round-bottomed flask equipped with a condenser, acetylacetone (29.3 g, 0.29 mol) and N,N -diethylethylenediamine (34 g, 0.29 mol) in benzene (250 mL) were heated to reflux for 48 h to yield an intense yellow solution. The conversion was monitored by measurement of the water removed from the reaction through a Dean–Stark apparatus. The reaction starts immediately, as suggested by the color change, but it was necessary to heat to reflux for 2 d to complete it. The solvent was then removed to yield an intense yellow liquid. Distillation at 145 °C yielded the product as a yellow oil. Yield: 49.7 g (87.6%). ^1H NMR (C_6D_6 , 300 MHz): δ = 11.1 (s, 6 H, $\text{CH}_3\text{CCHCCH}_3$), 2.93 (q, J = 6.2 Hz, 2 H, NHCH_2CH_2), 2.37 [q, J = 7.2 Hz, 4 H, $\text{N}(\text{CH}_2\text{CH}_3)_2$], 2.34 (t, J = 6.6 Hz, 2 H, NHCH_2CH_2), 2.08 (s, 3 H, CH_3CO), 1.64 (s, 3 H, CH_3CN), 0.98 [t, J = 7 Hz, 6 H, $\text{N}(\text{CH}_2\text{CH}_3)_2$] ppm. $^{13}\text{C}\{^1\text{H}\}$ NMR (C_6D_6 , 75.47 MHz): δ = 193.5, 161.4, 95.0, 52.9, 47.3, 41.5, 28.7, 18.5, 12.1 ppm.

Synthesis of Compound 1: A solution of HL^1 (7.5 g, 0.038 mol in 10 mL of THF) was added to a solution of CuCl_2 (5 g, 0.038 mol) in THF (10 mL), followed by stirring at room temperature for 1 h. The solution became dark green. Then Et_3N (5.5 mL, 0.04 mol) was added, followed by stirring for another 1 h, resulting in the formation of a white precipitate ($\text{Et}_3\text{NH}^+\text{Cl}^-$), which was removed by filtration. The solvent was partially removed under reduced pressure to about 5 mL, and slow diffusion of hexane gave black crystals suitable for analysis and for the X-ray diffraction analysis. Yield: 9.1 g (98.1%). $\text{C}_9\text{H}_{17}\text{ClCuN}_2\text{O}$: calcd. C 40.30, H 6.39, N 10.44; found C 39.6, H 6.8, N 10.3. EPR (CH_2CH_2 , room temp.): g = 2.097; a_{Cu} = 83.4 G. EPR (CH_2CH_2 , 120 K): g_{\parallel} = 2.20 (a_{\parallel} \approx 190 G), g_{\perp} = 2.08.

Synthesis of Compound 2: A solution of HL^2 (6.5 g, 0.038 mol in 10 mL of THF) was added to a solution of CuCl_2 (5 g, 0.038 mol) in THF (10 mL), followed by stirring at room temperature for 1 h. The solution became dark green. Then Et_3N (5.5 mL, 0.04 mol) was added, followed by stirring for another 1 h, resulting in the formation of a white precipitate ($\text{Et}_3\text{NH}^+\text{Cl}^-$), which was removed by filtration. The solvent was partially removed under reduced pressure to about 5 mL, and slow diffusion of hexane gave black crystals suitable for analysis. Yield: 4.8 g (57.9%). $\text{C}_{11}\text{H}_{21}\text{ClCuN}_2\text{O}$: calcd. C 44.59, H 7.14, N 9.45; found C 44.0, H 7.7, N 9.4. EPR (CH_2CH_2 , room temp.): g = 2.098; a_{Cu} = 81.4 G. EPR (CH_2CH_2 , 120 K): g_{\parallel} = 2.20 (a_{\parallel} \approx 180 G), g_{\perp} = 2.09.

Standard Procedure for the Polymerization Experiments: The polymerizations were conducted in predried Schlenk flasks. The solids (complexes, initiators, and bipyridine) and a stirring bar were added, and then the flask was sealed with a glass septum. Oxygen was removed from the flask by applying a vacuum and backfilling with argon (three cycles). The monomer and the solvents (pyridine, toluene, and dodecane) were added with a syringe. The solution was degassed by three freeze–pump–thaw cycles. A first sample was removed as reference and the flask immersed in an oil bath kept at the desired temperature by thermostat. At timed intervals, samples

were removed from the flask by syringe and diluted in THF. Each sample was filtered through neutral alumina to remove the catalyst. A small amount of this THF solution was used to determine the monomer conversion by gas chromatography (GS) with dodecane as an internal standard. From the remaining sample, the polymer product was precipitated by addition into an excess amount of MeOH. The precipitate was collected and analyzed by gel permeation chromatography (GPC).

X-ray Crystallography: A single crystal of each compound was mounted under inert perfluoropolyether on the tip of a glass fiber and cooled in the cryostream of either an Oxford-Diffraction XCALIBUR CCD diffractometer (for **1**) or an Oxford-Diffraction GEMINI CCD diffractometer (for **2**). Data were collected by using monochromatic Mo- K_{α} radiation (λ = 0.71073 Å) at 180(2) K. The structures were solved by direct methods (SIR97)^[45] and refined by least-squares procedures on F^2 using SHELXL-97.^[46] All H atoms attached to carbon atoms were introduced in calculated idealized positions and treated as riding models. The drawing of the molecules was realized with the help of ORTEP32.^[47] The crystal data and structure refinement parameters for both compounds are listed in Table 1.

Table 1. Crystal data for compounds **1** and **2**.

Compound	1	2
Empirical formula	$\text{C}_9\text{H}_{17}\text{ClCuN}_2\text{O}$	$\text{C}_{11}\text{H}_{21}\text{ClCuN}_2\text{O}$
M_r	268.24	296.30
Crystal system	monoclinic	monoclinic
Space group	$P2_1/n$	$P2_1/n$
a [Å]	10.2397(4)	10.2616(3)
b [Å]	9.6133(4)	9.7014(3)
c [Å]	12.3296(5)	14.1431(4)
α [°]	110.201(4)	103.053(3)
V [Å ³]	1139.03(8)	1371.59(7)
Z	4	4
$D_{\text{calcd.}}$ [Mg m ^{−3}]	1.564	1.435
Abs. coeff. [mm ^{−1}]	2.122	1.770
$F(000)$	556	620
Crystal size [mm]	0.12 × 0.11 × 0.07	0.44 × 0.34 × 0.31
θ range [°]	2.75–28.32	3.48 to 29.12
Reflections collected	12338	15349
Unique reflections [$R(\text{int})$]	2646 (0.0266)	3263 (0.0228)
Completeness [%]	93.3	94.2
Absorption correction	multiscan	multiscan
Max./min. transmission	1.00000/0.74280	1.00000/0.86185
Refinement method	F^2	F^2
Data/restraints/parameters	2416/0/131	3204/0/149
Goodness-of-fit on F^2	1.101	1.103
R , $wR2$ [$I > 2\sigma(I)$]	0.0224, 0.0601	0.0217, 0.0607
R , $wR2$ (all data)	0.0264, 0.0616	0.0289, 0.0619
Residual density [e Å ^{−3}]	0.287, −0.611	0.415, −0.269

CCDC-800731 (for **1**) and -800732 (for **2**) contain the supplementary crystallographic data for this paper. These data can be obtained free of charge from The Cambridge Crystallographic Data Centre via www.ccdc.cam.ac.uk/data_request/cif.

Supporting Information (see footnote on the first page of this article): Tables of conversions, molecular weights, and polydispersity index for the all polymerization experiments.

Acknowledgments

We are grateful to the Agence National de la Recherche (Programme ANR Blanc “OMRP,” 2010–13), the Centre National de

la Recherche Scientifique (CNRS), and the Institut Universitaire de France (IUF) for support of this work and to the Politecnico, Milan, Italy for an Erasmus exchange fellowship to S. G. We also thank Dr. Zhigang Xue and Mr. Andrés F. Cardozo for technical assistance.

- [1] J.-S. Wang, K. Matyjaszewski, *J. Am. Chem. Soc.* **1995**, *117*, 5614–5615.
- [2] K. Matyjaszewski, J. H. Xia, *Chem. Rev.* **2001**, *101*, 2921–2990.
- [3] M. Kamigaito, T. Ando, M. Sawamoto, *Chem. Rev.* **2001**, *101*, 3689–3745.
- [4] M. Ouchi, T. Terashima, M. Sawamoto, *Chem. Rev.* **2009**, *109*, 4963–5050.
- [5] F. Di Lena, K. Matyjaszewski, *Prog. Polym. Sci.* **2010**, *35*, 959–1021.
- [6] T. Pintauer, K. Matyjaszewski, *Coord. Chem. Rev.* **2005**, *249*, 1155–1184.
- [7] M. Munakata, S. Kitagawa, A. Asahara, H. Masuda, *Bull. Chem. Soc. Jpn.* **1987**, *60*, 1927–1929.
- [8] M. Becker, F. W. Heinemann, S. Schindler, *Chem. Eur. J.* **1999**, *5*, 3124–3129.
- [9] N. Kitajima, K. Fujisawa, Y. Morooka, *J. Am. Chem. Soc.* **1990**, *112*, 3210–3212.
- [10] C. Mealli, C. S. Arcus, J. L. Wilkinson, T. J. Marks, J. A. Ibers, *J. Am. Chem. Soc.* **1976**, *98*, 711–718.
- [11] J. S. Thompson, R. L. Harlow, J. F. Whitney, *J. Am. Chem. Soc.* **1983**, *105*, 3522–3527.
- [12] Q. Zhao, W.-L. Cao, Z.-Y. Yang, J.-C. Zhang, *Beijing Huagong Daxue Xuebao, Ziran Kexueban* **2005**, *32*, 68–71.
- [13] S. H. Hsu, C. Y. Li, Y. W. Chiu, M. C. Chiu, Y. L. Lien, P. C. Kuo, H. M. Lee, J. H. Huang, C. P. Cheng, *J. Organomet. Chem.* **2007**, *692*, 5421–5428.
- [14] A. F. Lugo, A. F. Richards, *Inorg. Chim. Acta* **2010**, *363*, 2104–2112.
- [15] X. Zhang, H. Bian, W. Gu, F. Huang, S. Yan, H. Liang, *Nankai Daxue Xuebao, Ziran Kexueban* **2009**, *42*, 59–63.
- [16] M. Becht, T. Gerfin, K. H. Dahmen, *Helv. Chim. Acta* **1994**, *77*, 1288–1298.
- [17] H. Y. Tang, H. Y. Chen, J. H. Huang, C. C. Lin, *Macromolecules* **2007**, *40*, 8855–8860.
- [18] C. Biswas, M. G. B. Drew, A. Ghosh, *Inorg. Chem.* **2008**, *47*, 4513–4519.
- [19] A. F. Lugo, A. F. Richards, *Eur. J. Inorg. Chem.* **2010**, 2025–2035.
- [20] L. A. Lesikar, A. F. Gushwa, A. F. Richards, *J. Organomet. Chem.* **2008**, *693*, 3245–3255.
- [21] Y. M. Chumakov, M. D. Mazus, V. N. Biyushkin, N. I. Belichuk, T. I. Malinovskii, *Izv. Akad. Nauk Mold. SSR, Ser. Fiz.-Tekh. Mater. Nauk* **1979**, 83–86.
- [22] V. K. Kravtsov, V. N. Biyushkin, L. A. Nezhelskaya, T. I. Malinovskii, *Koord. Khim.* **1993**, *19*, 235–239.
- [23] M. E. Bluhm, M. Ciesielski, H. Görls, O. Walter, M. Döring, *Inorg. Chem.* **2003**, *42*, 8878–8885.
- [24] E. Gyepes, E. Kuchar, A. Jurikova, *Acta Fac. Rerum Nat. Univ. Comenianae, Chim.* **1981**, *29*, 69–80.
- [25] J. M. Latour, S. S. Tandon, G. A. Leonard, D. C. Povey, *Acta Crystallogr., Sect. C: Cryst. Struct. Commun.* **1989**, *45*, 598–600.
- [26] F. Hueso-Urena, M. N. Moreno-Carretero, A. L. Penas-Chamorro, J. M. Amigo, V. Esteve, T. Debaerdemaecker, *Polyhedron* **1999**, *18*, 3629–3636.
- [27] C. T. Zeyrek, A. Elmali, Y. Elerman, *Z. Naturforsch. B* **2006**, *61*, 237–242.
- [28] J. C. Ma, J. Yang, J. F. Ma, *Acta Crystallogr., Sect. E: Struct. Rep. Online* **2007**, *63*, M2431–U1649.
- [29] X. Y. Ma, X. D. Dong, Y. P. Li, Z. G. Zhang, *Acta Crystallogr., Sect. E: Struct. Rep. Online* **2007**, *63*, M1729–U1327.
- [30] A. M. Prokhorov, P. A. Slepukhin, D. N. Kozhevnikov, *J. Organomet. Chem.* **2008**, *693*, 1886–1894.
- [31] B. Sarkar, G. Bocelli, A. Cantoni, A. Ghosh, *J. Coord. Chem.* **2008**, *61*, 3693–3702.
- [32] N. A. I. Hisham, H. M. Ali, S. W. Ng, *Acta Crystallogr., Sect. E: Struct. Rep. Online* **2009**, *65*, M870–U453.
- [33] K. D. Onuska, N. J. Taylor, J. Carsky, *J. Chem. Crystallogr.* **1996**, *26*, 841–846.
- [34] U. Sandbhor, S. Padhye, D. Billington, D. Rathbone, S. Franzblau, C. E. Anson, A. K. Powell, *J. Inorg. Biochem.* **2002**, *90*, 127–136.
- [35] R. Kannappan, S. Tanase, I. Mutikainen, U. Turpeinen, J. Reedijk, *Inorg. Chim. Acta* **2005**, *358*, 383–388.
- [36] R. Karmakar, C. R. Choudhury, A. S. Batsanov, S. R. Batten, S. Mitra, *Struct. Chem.* **2005**, *16*, 535–539.
- [37] S. Das, S. A. Maloor, S. Pal, *Cryst. Growth Des.* **2006**, *6*, 2103–2108.
- [38] P. U. Maheswari, S. Roy, H. Den Dulk, S. Barends, G. Van Wezel, B. Kozlevcar, P. Gamez, J. Reedijk, *J. Am. Chem. Soc.* **2006**, *128*, 710–711.
- [39] P. Barbazan, R. Carballo, E. M. Vazquez-Lopez, *CrytEngComm* **2007**, *9*, 668–675.
- [40] A. Ray, G. Pilet, C. J. Gomez-Garcia, S. Mitra, *Polyhedron* **2009**, *28*, 511–520.
- [41] H. Elias, E. Hilms, H. Paulus, *Z. Naturforsch. B* **1982**, *37*, 1266–1273.
- [42] J. Wang, Z. You, *Acta Crystallogr., Sect. E: Struct. Rep. Online* **2007**, *63*, M1200–M1201.
- [43] A. N. Shnulin, Y. T. Struchkov, K. S. Mamedov, A. A. Medzhidov, T. M. Kutovaya, *J. Struct. Chem.* **1977**, *18*, 799–805.
- [44] R. Gebbink, M. Watanabe, R. C. Pratt, T. D. P. Stack, *Chem. Commun.* **2003**, 630–631.
- [45] A. Altomare, M. Burla, M. Camalli, G. Casciarano, C. Giacovazzo, A. Guagliardi, A. Moliterni, G. Polidori, R. Spagna, *J. Appl. Crystallogr.* **1999**, *32*, 115–119.
- [46] G. M. Sheldrick, *Acta Crystallogr., Sect. A: Found. Crystallogr.* **2008**, *64*, 112–122.
- [47] L. J. Farrugia, *J. Appl. Crystallogr.* **1997**, *30*, 565.

Received: November 15, 2010

Published Online: February 23, 2011